Bull. Fac. Bioresources, Mie Univ.
No. 3: 25–39
February 28. 1990

A Barotropic Numerical Model for the Wind-driven Circulation in the Okhotsk Sea

Yoshihiko SEKINE

Faculty of Bioresources, Mie University

Wind-driven circulation in the Okhotsk Sea is studied by use of a barotropic numerical model. The monthly mean wind stress over the period of 1961–1975 provided by Kutsuwada and Sakurai[1] is used. It is shown that a prominent flow in the Okhotsk Sea is confined to the slope region around the deep Kuril Basin by the bottom topographic effect. It is also pointed out that the wind-driven circulation is very weak in summer, but strong in winter, which suggests that the wind-driven circulation dominates in winter, while the circulation is due to in- and outflow in summer. To see the effect of ice cover in winter, a model with the wind stress only imposed over the open sea region is examined. This model shows that although the flow is weak in the northern marginal region, the remarkable wind-driven circulation is formed in most of the basin by the propagation of the Rossby wave.

Key words: numerical model, wind-driven circulation, the Okhotsk Sea

1. Introduction

The Okhotsk Sea is a marginal Sea in the north Pacific. The major feature of the current system in the Okhotsk Sea is the in- and outflow of the Oyashio and the Soya Warm Current; the Oyashio flows into the Okhotsk Sea through the Onnekotan and Mushiru Straits in the Kuril Islands and flows out through the southwestern straits in the Kuril Islands[2] (cf. Fig. 1 (a)). The Soya Warm Current enters throught the Soya Strait and flows out through the Kunashiri Strait. So far, there have been many reports on the Soya Warm Current.[3),4),5)]

However, the observational study on the general circulation in the Okhotsk Sea has not been carried out well. A few observational evidences are described.[6),7)] Because the Okhotsk Sea is rather shallow, the tidal current may be prominent in the current system.[8)] Another characteristic feature of the Okotsk Sea is a surface freezing in winter. The open sea (ice-free region) is found in southeatern region of the Kamchatka Pen. So, the surface freezing is considered to give serious influences on the wind-driven circulation in the Okhotsk Sea.

In the present study, the wind-driven cirulation in the Okhotsk Sea is examined as the initial phase of this study by using a barotropic model and historical wind stress data.[1)] Especially, we investigate the characteristics of the in- and outflow of the Oyashio through the Kuril Islands and of the Soya Warm Current, the topographic effect of the Kuril Basin and the seasonal change in the wind-driven circulation in the Okhotsk Sea.

Received March 10, 1989

2. The Model

The schematic view of the model ocean is shown in Fig. 1 (b). Coastal topograpgy is simplified so that only the main features are modeled. To see the specifed effect of the bottom topography, two models with different bottom topographies are performed (see, Fig. 2). The orthogonal coordinates are taken as in Figs. 1 (b) and 2.

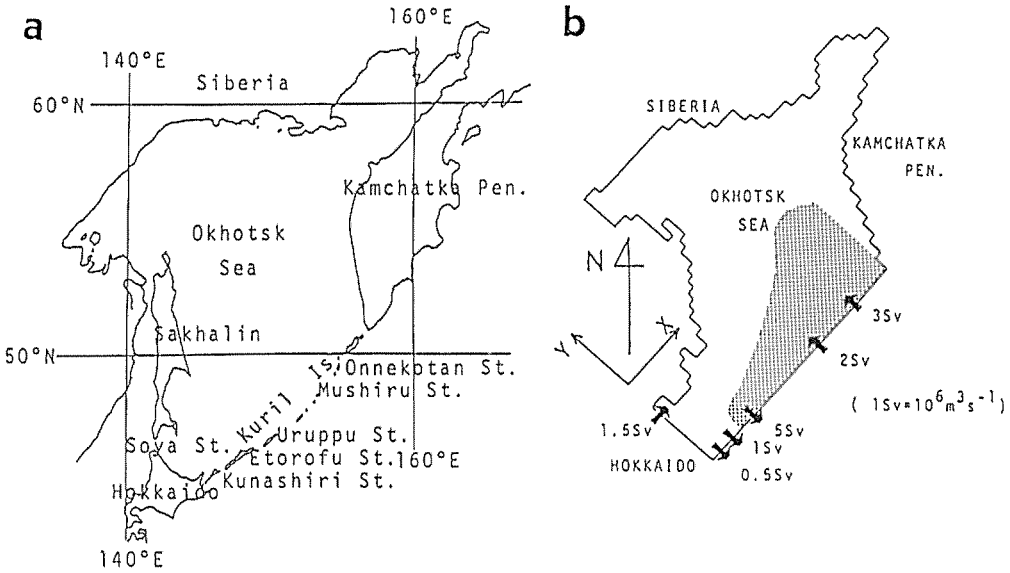

Fig. 1. (a) Map of the Okhotsk Sea and (b) top view of the model ocean, in which an open sea region assumed in the present study is stippled.

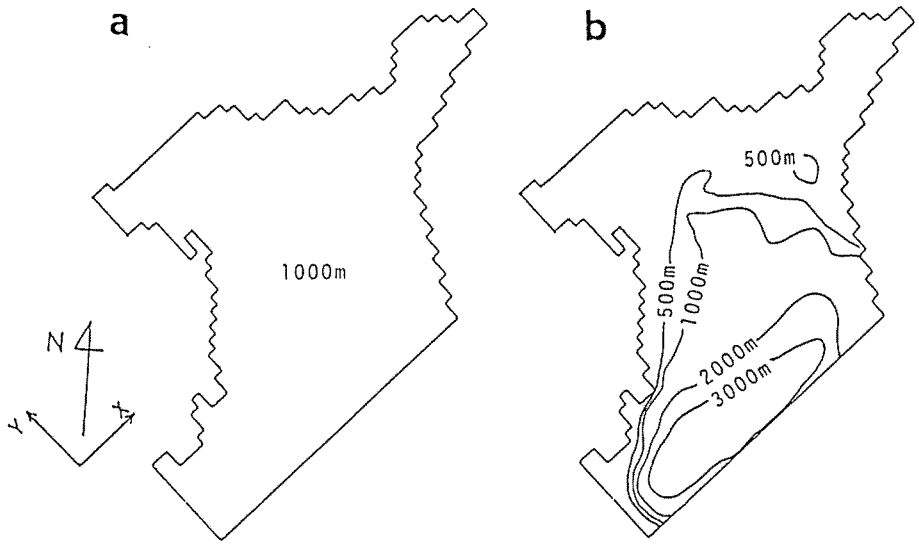

Fig. 2. Two cases of the top view of the model ocean, (a) a flat bottom model with a depth of 1000 m and (b) a simplified bottom model.

The angle between x axis (y axis) and eastward (northward) is 45°. The basic equations under hydrostatic, the β-plane and rigid lid approximations are as follows[9]:

$$\frac{\partial z}{\partial t}+\frac{\partial uz}{\partial x}+\frac{\partial vz}{\partial y}+\beta_x u+\beta_y v+f\left(\frac{\partial u}{\partial x}+\frac{\partial v}{\partial y}\right)=A_h\nabla^2 Z+curl\left(\frac{\tau}{h}\right), \tag{1}$$

where

$$z=\frac{\partial v}{\partial x}-\frac{\partial u}{\partial y}. \tag{2}$$

$$u=-\frac{1}{h}\frac{\partial \phi}{\partial y},\quad v=\frac{1}{h}\frac{\partial \phi}{\partial x}. \tag{3}$$

The notations used in the above equations have the folowing meanings:

- t : time (sec)
- u, v : horizontal component of the velocity in the x- and y- directions (cm sec^{-1})
- h : depth of the ocean (cm)
- z : relative vorticity (sec^{-1})
- ϕ : volume transport function (cm^3 sec^{-1})
- f : Coriolis parameter ($f=f_0+\beta_x x+\beta_y y$, $f_0=9.91\times10^{-5}sec^{-1}$) ($sec^{-1}$)
- β_x, β_y : constant change rate of the Coriolis parameter ($\beta_x=\beta_y=1.41\times10^{-13}$ $cm^{-1}sec^{-1}$)
- τ : wind stress vector (dyn cm^{-2})
- ∇^2 : Laplacian operator for the horizontal direction
- A_h : constant coefficient of horizontal eddy viscosity (cm^2 sec^{-1})

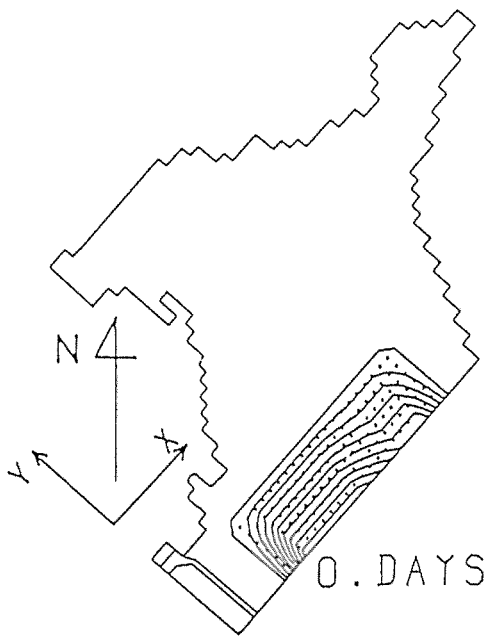

Fig. 3. Initial condition of the volume transport function. Contour interval is 0.5 Sv (1 Sv=10^{12} cm^3sec^{-1})

The equations (1) and (2)–(3) are solved numerically with the grid resolution of 41.87 km. A leap frog scheme is basically used in the finite form of the local change and additionaly an Euler backward scheme[10] at every 20 time step is employed to suppress the growth of computational modes. Viscous lateral boundaries are set up. On the basis of the gross feature of the observational evidences[3], two in-and outflows of 5 Sv (1 Sv= 10^{12} cm^3sec^{-1}) corresponging to the Oyashio and 1.5 Sv to the Soya Warm Current is given at the boundary (see, Fig. 1 (b)). The initial condition of the volume transport function is shown in Fig. 3.

In order to see the specified roles of bottom topography and wind stress, nineteen runs with different model characteristics are performed (see Table). In the first phase (Runs 1–4), the dependence on the horizontal eddy ciscosity is checked by use of a flat bottom model shown in Fig 2 (a). No wind stress is imposed in these runs and character of the circulation induced by the in- and outflow is examined. In the second phase (Runs 5–9), a seasonally averaged constant wind stress is imposed. In particular, the effect of the surface freezing in winter is examined in Run 9, by imposing the wing stress only over the open sea shown by the stippled area in Fig. 1 (b). Although there exist some effects of the wind stress depending on the condition of the sea ice, these parameterizations are left out the future study. In the third phase, runs similar to the second phase but for the simplified bottom topography (Fig. 2 (b)) are tried. These runs are employed to see the effect of bottom on the circulation in the Okhotsk Sea.

Table Wind stress, bottom topography and coefficient of of horizontal eddy viscosity for the experiments. Blank indicates no change from Run 1.

Run no.	Wind stress	Bottom topography	COefficient of eddy viscosity (cm^2s^{-1})	Remarks
1	no	flat	5×10^6	basic model
2			5×10^7	viscosity
3			1×10^6	〃
4			5×10^5	〃
5	spring wind stress			wind stress
6	summer wind stress			〃
7	autumn wind stress			〃
8	winter wind stress			〃
9	winter wind stress over the open sea			wind stress & sea ice effect
10		realistic		bottom topography
11	spring wind stress	realistic		wind stress & bottom topography
12	summer wind stress	realistic		〃
13	autumn wind stress	realistic		〃
14	winter wind stress	realistic		〃
15	winter wind stress over the open sea	realistic		wind stress, bottom topography & sea ice effect.
16				observed in-and outflow
17		realistic		observed in-and outflow & bottom topography
18	summer wind stress			observed in-and outflow & wind stress.
19	summer wind stress	realistic		observed in-and outflow wind stress & bottom topography.

The steady in-and outflow is given all the previous runs, however, there is a seasonal variation of the in- and outflow of the Okhotsk Sea. Unfortunately, few observational data are available except for summer. Therefore, in the last phase, the observed in- and outflow in summer is given at the boundary and four different models (Runs 16–19) are examined: two no wind cases with a different bottom topography (Runs 16 and 17) and the other two cases with the summer wind stress (Runs 18 and 19) are performed.

3. Wind stress data

The wind stress used in the present study is shown in Fig. 4. Wind stresses in winter, spring, summer

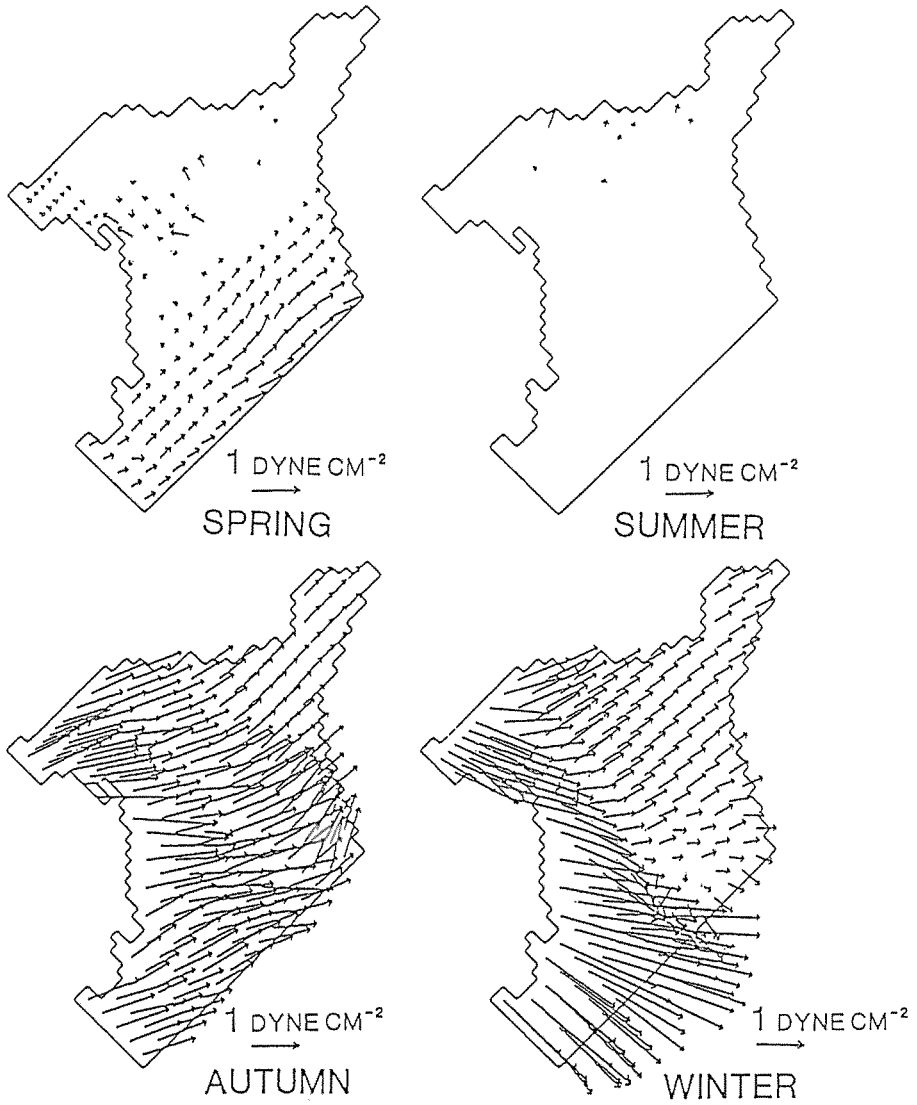

Fig. 4. Seasonally averaged wind stress vectors used in the numerical model.[1] No value below 0.05 dyne cm^{-2} is plotted.

and autumn are estimated by the average of two monthly mean data of January and February, April and May, July and August, October and November, respectively by use of wind stress data.[1] Fig. 4 shows that, in summer, wind is very weak. But the wind is strong in autumn and winter. Westerly wind is dominant in autumn and northwesterly wind monsoon prevails in winter.

Vertical component of curl τ (τ is the wind stress vector) is shown in Fig. 5. In all seasons, complicated curl τ distributions are found. An positive curl region in the center of the model ocean in autumn, and complicated strong positive and negative curl τ distribution in winter are particularly noticed.

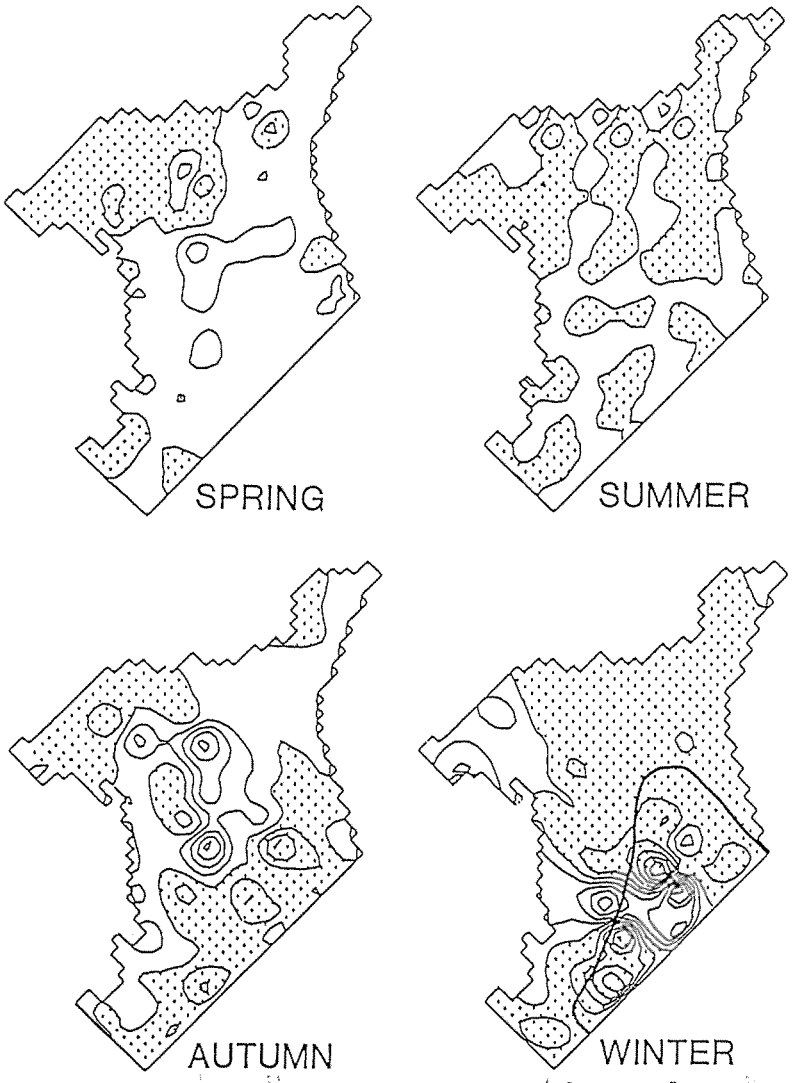

Fig. 5. Curl of the wind stress in Fig. 4. Contour interval is 10^{-9} dyne cm^{-3} and the negative curl regions are dotted. Heavy solid line in the winter panel shows the boundary of the open sea shown in Fig 1 (b).

4. Results

Firstly, we see the characteristics of the circulation generated by in-and outflow of the Oyashio and the Soya Warm Current calculated in the two basic models with no wind stress. The time change in the volume transport functions of Runs 1 with a flat bottom and Run 10 with a simplified bottom of the Okhotsk Sea are shown in Fig. 6. In Run 1, the in- and outflow corresponding to the Oyashio forms a western boundary current along southern coast of Sakhalin and northeastern coast of Hokkaido. A clear cyclonic circulation is formed in the Okhotsk Sea. The cyclonic circulation is almost confined to south of the inflow boundary latitude as the results of zonal propagation of the Rossby wave. In contrast to this, the flow pattern in Run 10 is quite different; the inflow has a tendency to flow along the isopleth of the depth and a western boundary current formed in Run 1 is not formed in Run 10. The predominant circulation is mainly confined to the slope region around the Kuril Basin. For both runs, no major variation in the flow patterns occurrs after 60 days and it shows that a quasi-stationary state is attained in about two months.

Secondly, the model dependence on the intensity of the horizontal eddy viscosity is checked in Fig. 7. In these three models, almost similar flow patterns are found in Runs 3 ($A_h=10^6$ cm^{2}sec^{-1}) and 4 ($A_h=5\times10^5$

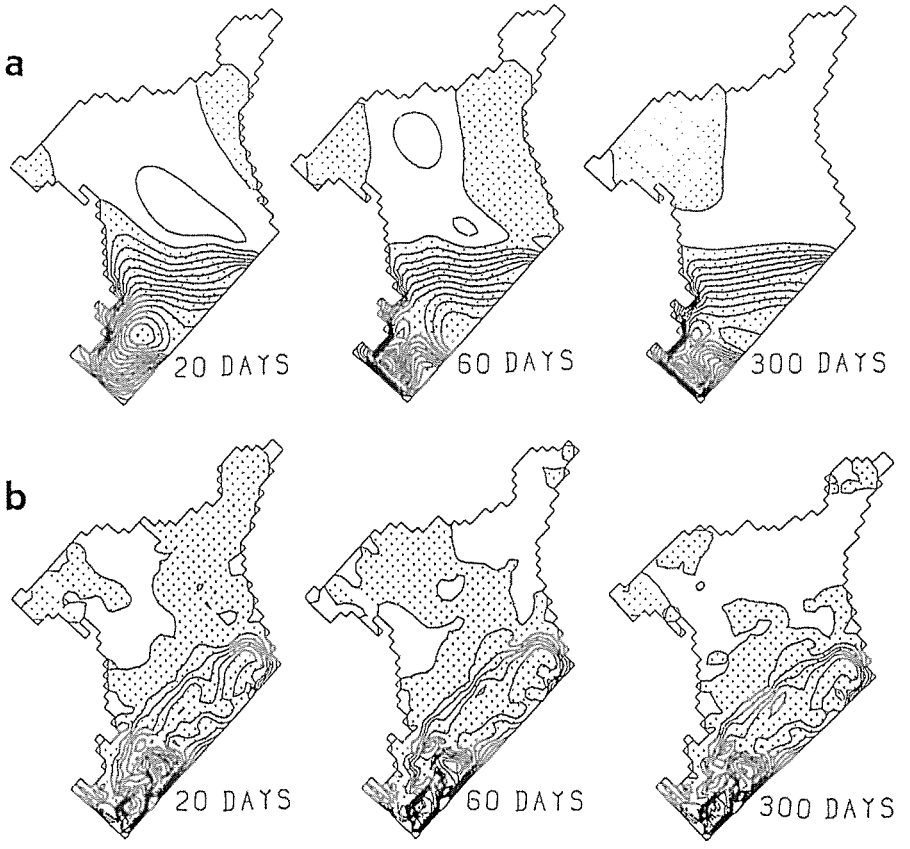

Fig. 6. Sequential patterns of the volume transport function (a) Run 1 and (b) Run 10. Contour interval is 0.5 Sv and regions with the negative volume transport function are dotted.

cm^2sec^{-1}). However, the flow pattern of Run 2 ($A_h=5\times10^7$ cm^2sec^{-1}) is different and it resembles Munk solution.[11] The width of the boundary current of Run 2 is wider than those of Runs 3 and 4, in which eddylike flow patterns are more remarkable. If we compare the results of Run 1 shown in Fig. 6 (a) with those of Fig. 7, it is noted that the flow pattern of Run 1 is almost similar to Runs 3 and 4, except for a small suppression of the eddy effect. On the basis of minor dependence of the flow patterns on the intensity of eddy viscosity between Run 1 and Runs 3 and 4 with the smaller eddy viscosity, constant coefficient of eddy viscosity of Run 1 (5×10^6 cm^2sec^{-1}) is used in the following models with the seasonally averaged wind stress.

The quasi-stationary state of Runs 5–9 with a flat bottom are shown in Fig. 8. In spring (Run 5), the prominent southward western boundary current is formed along the eastern coast of Sakhalin and the inner cyclonic circulation has a transport of 5 Sv, which is approximately as much as the given inflow of the Oyashio. Wind-driven circulation is rather small in the southern region (see, Fig 8 (b)). In summer (Run 6), the wind-driven circulation is very weak and the dominant current is the in-and outflow of the Oyashio through the Kuril Islands. The constant in- and outflow with the transport of 5 Sv is assumed in the model, and it is suggested that the actual circulation in summer is more influenced by the in- and outfiow. If the in- and outflow is very small, the total flow pattern is approximated by the solution shown in Fig. 8 (b), in which only a weak anticyclonic circulation is formed along the northern boundary. In autumn (Run 7), the wind-driven circulation recovers. In particular, a cyclonic circulation with the southward western boundary current is formed in north of the Sakhalin. In contrast to this, an anticycloic circulation is formed in the southern basin and it yields the

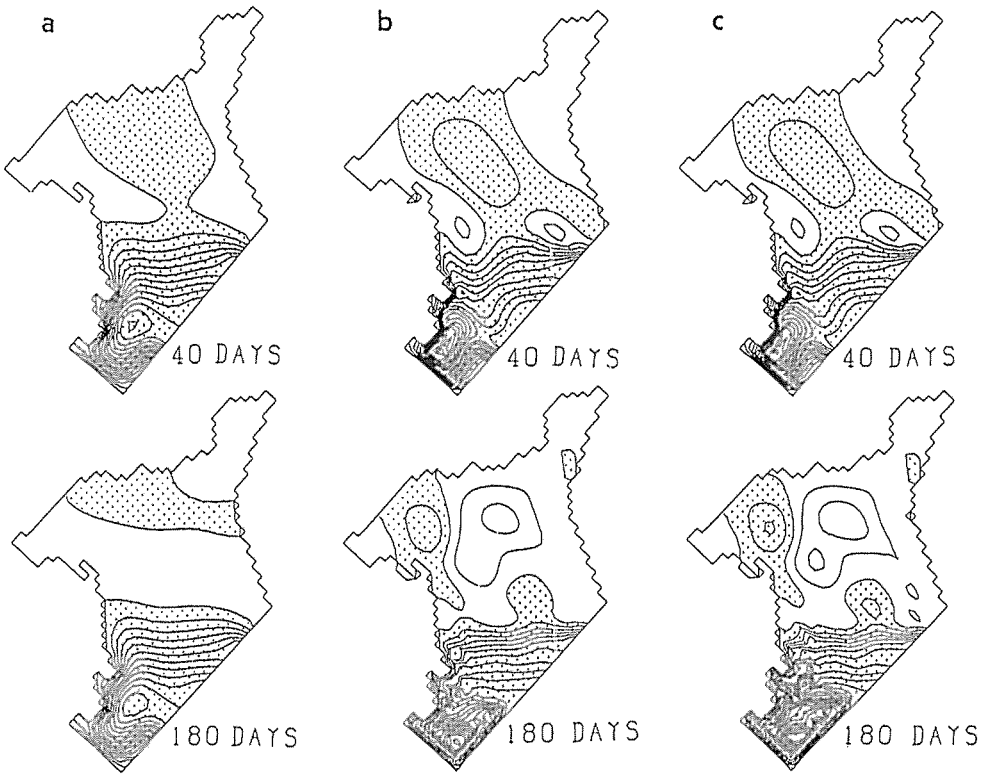

Fig. 7. Same as in Fig. 6, but for (a) Run 2, (b) Run 3 and (c) Run 4.

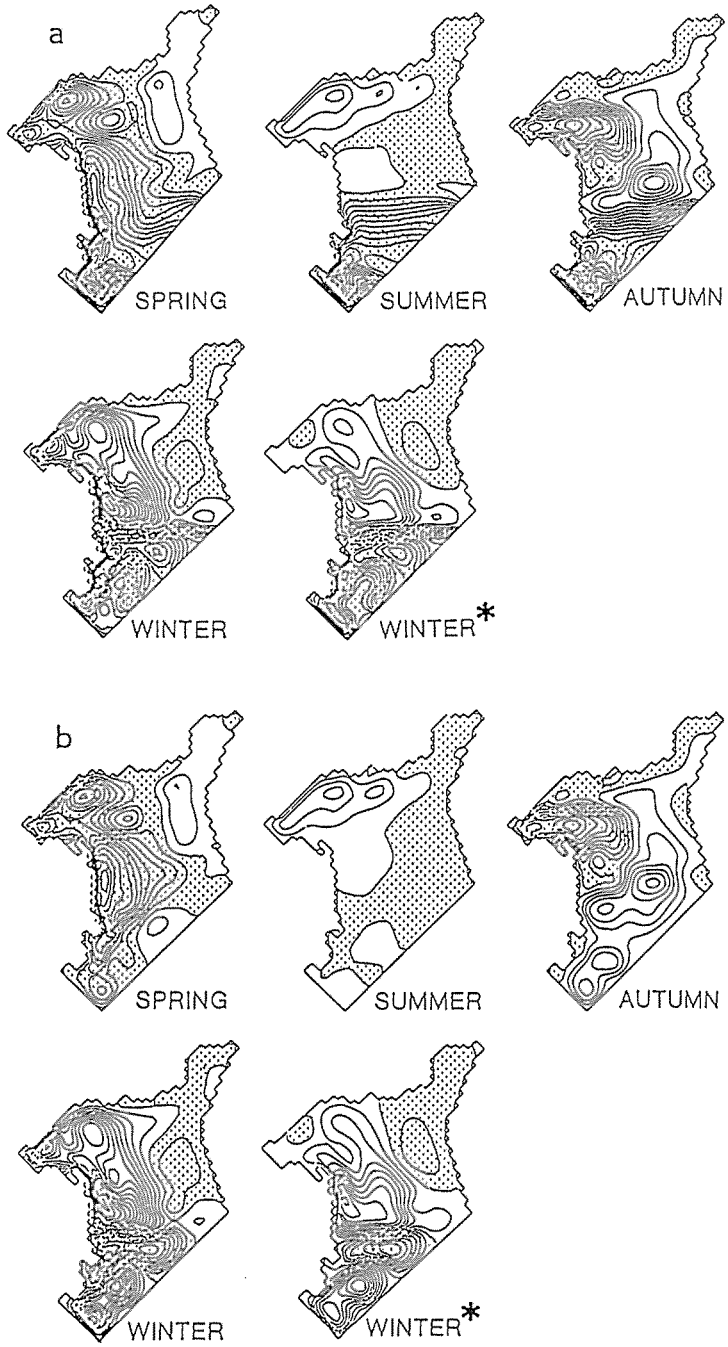

Fig. 8. (a) Same as in Fig. 6, but for flat models with seasonally mean wind stress. (b) Wind-driven circulation component in (a) evaluated by subtracting the volume transport function of Run 1 from that of each Run. Panels marked by spring, summer, autumn, winter and winter* show the quasi-stationary state of Run 5, Run 6, Run 7, Run 8 and Run 9, respectively.

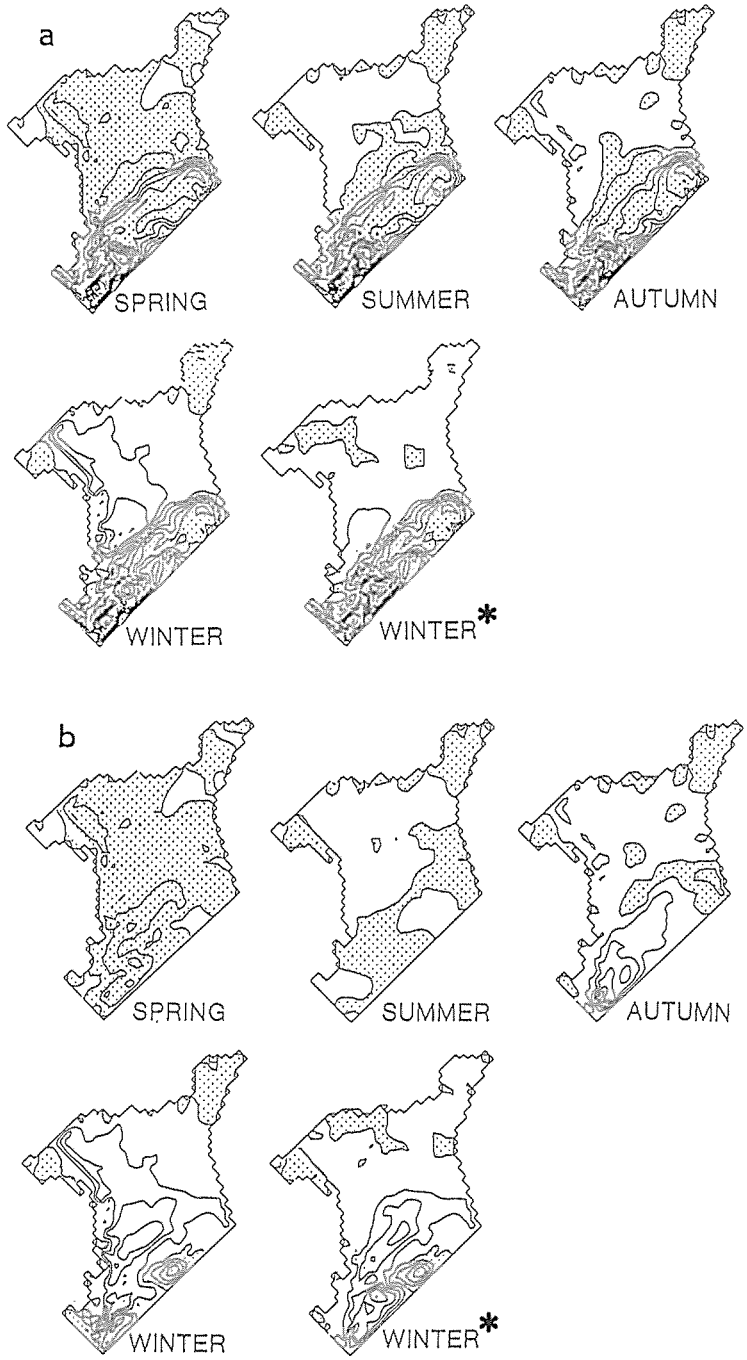

Fig. 9. (a) Same as in Fig. 8, but for models with the simplified bottom topograpgy. (b) Wind-driven circulation component in (a). Panels marked by spring, summer, autumn, winter and winter* show the quasi-stationary state of Run 11, Run 12, Run 13, Run 14 and Run 15, respectively.

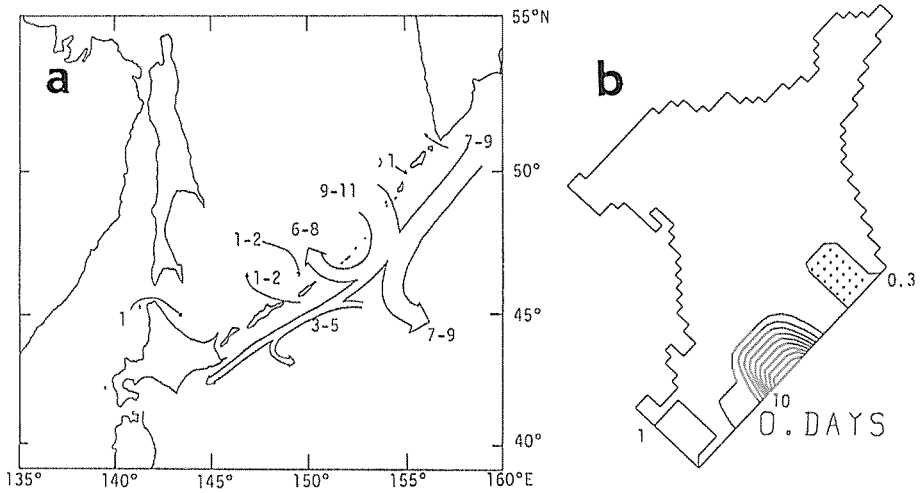

Fig. 10. (a) Observed volume transport in summer estimated by the geostrophic calculation referred to 1000 db.[13]
(b) Initial condition of the volume transport function for Runs 16-19. Contour interval is 1 Sv.

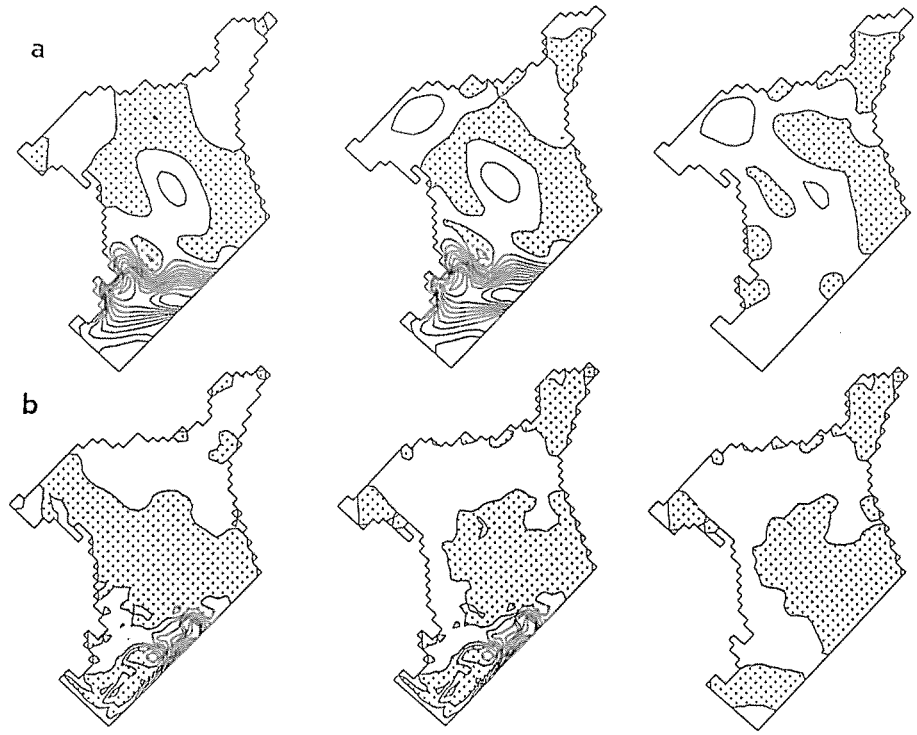

Fig. 11. Quasi-stationary flow pattern of Runs 16–19 shown by the volume transport function. (a) Run 16 (left), Run 18 (center) and wind-driven circulation component of Run 18 (right). (b) Run 17 (left), Run 19 (center) and wind-driven circulation component of Run 19 (right). Contour interval is 1 Sv.

northward western boundary current off Hokkaido and off southern Sakhalin (see, Fig. 8 (b)). Because the anticyclonic circulation has just the opposite circulation to the cyclonic circulation formed by the in- and outflow of the Oyashio, the western boundary current is weak along southeastern region off Sakhalin. In winter (Run 8), a wind-driven circulation is very strong. An anticylonic circulation develops in the northern basin and a very complicated flow pattern is found in the southern basin. The wind-driven circulation in the Kuril Basin is anticylonic and it generates very weak western boundary flow off Soya Current. It is suggested from Runs 7 and 8 that interaction between the two circulations formed by the in-and outflow and by the wind-driven circulation is important for the circulation in a marginal sea. The similar relationship between the in-and outflow and the wind-driven circulation was pointed out in the circulation of the Japan Sea.[12)]

If the effect of the ice coverage is included (Run 9), the circulation is not remarkable in the northern region in comparison with Run 8. However, the flow is developed in almost of the southern basin. This is due to the propagation of the planetary Rossby wave and it suggests that the wind stress distribution in the open sea controls wind-driven circulation in the Okhotsk Sea. Because two positve wind stress curl region in the northwestern region and in the eastern off of Sakhalin are not covered by the open sea (see Fig. 5), the anticyclonic circulation is relatively weak in Run 9. Because the wind-driven circulation is very strong in winter, wind stress distribution over the open sea area is important for the general circulation in the Okhotsk Sea.

The quasi-stationary flow pattern of the models with the simplified bottom topography (Runs 11–15) are displayed in Fig. 9. The results has a clear contrast to the flat bottom cases shown in Fig. 8. By the effect of the inclined bottom topography, the volume transport in the northern half basin is decreased remarkably. The relatively large flow is found in the southern region, and the wind-driven circulation is very weak in all seasons. It is also shown from Fig. 9 (b) that the wind-driven circulation is confined to the deep region in the Kuril Basin and it has no interaction with the Soya Warm Current flowing in the shallower region.

Fig. 10 (a) shows the observed volume transport in summer estimated by the geostrophic calculation referred to 1000 db.[13)] It is shown that the major inflow and outfiow are carried out in the Uruppu St. and the Mushiru St., respectively. So the general feature in the in-and outflow pattern is quite different from the previous runs. The initial flow pattern based on the observational data is shown in Fig. 10 (b). The results of these runs are shown in Fig. 11. In flat bottom models (Runs 16 and 18), a clear anticyclonic circulation is formed in a southern region and a clear northward western boundary current is formed. As the wind stress is very weak in summer, the circulation is not changed by the imposition of the wind stress. In the cases with a simplified bottom topography shown in Fig. 11 (b), the topographic effect dominates and the main part of the inflow is confined to the southern Kuril Basin. In particular, the major inflow with the transport of 10 Sv flows out with a small anticyclonic circulation and it gives no influence on the general circulation. A cycloric circulation is formed in the southern part of the Kuril Basin by the topographic effect, which differs from those of flat bottom model. On the whole, it is pointed out that the circulation in the Okhotsk Sea is due to the in- and outflow in summer, in which the effect of the wind stress is very small.

5. Discussion

The numerical experiment for the wind-driven circulation in the Ohkotsk Sea was performed and some charactristic features werre obtained. On the whole, very clear seasonal change in the wind-driven circulation has been pointed out.

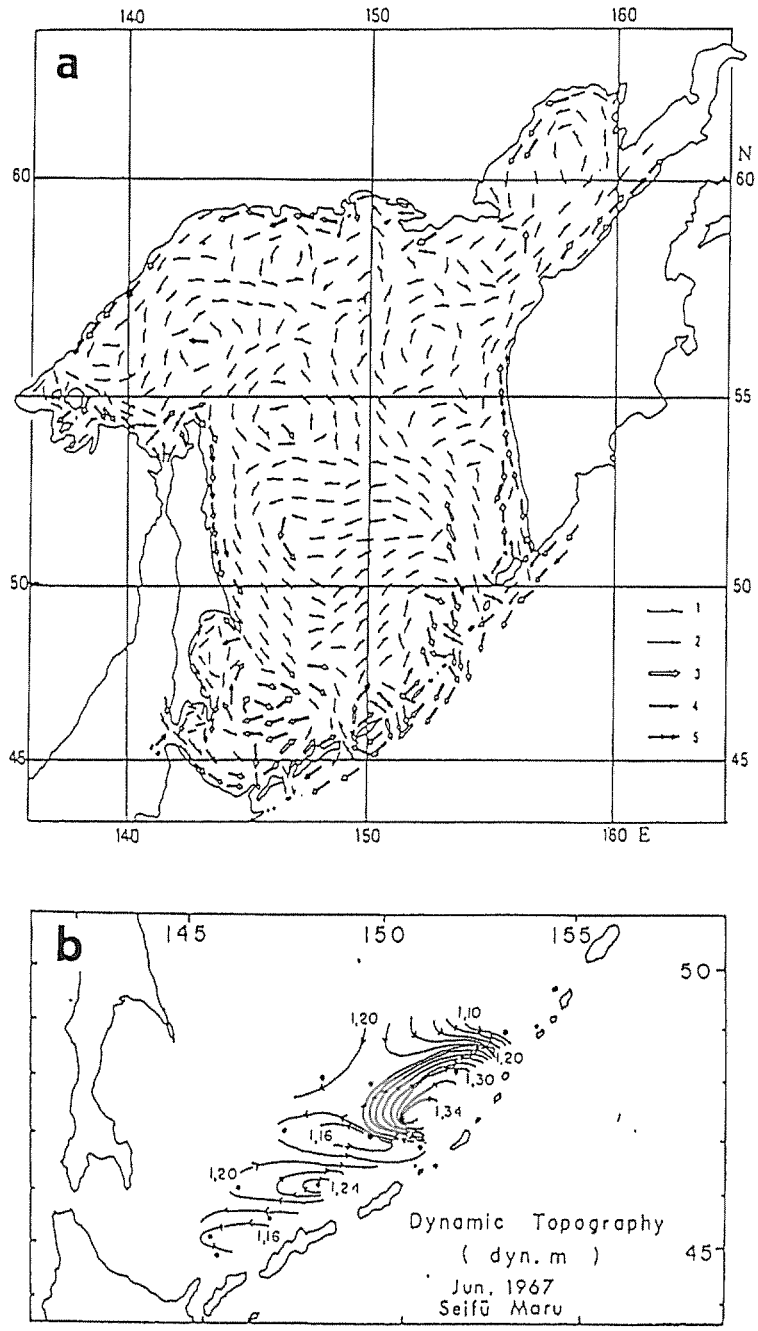

Fig. 12. (a) Surface current velocity in August estimated by the geostrophic balance referred to 2000 db.[14]

(b) Dynamic topography of the 400db layer with relative to 1500 db in June 1967.[7] Five kinds of arrows in (a) noted by 1, 2, 3, 4 and 5 show the current velocity <5 cms^{-1}, 5 cms^{-1}–10 cms^{-1}, 10 cms^{-1}–20 cms^{-1}, 20 cms^{-1}–30 cms^{-1} and 30 cms$^{-1}<$, respectively.

Although the clear observational features have not proposed yet, a surface geostrophic flow in August[14] and the dynamic topography of the 400 db layer referred to 1500 db in June[7] are displayed in Fig. 12. Relatively strong circulation are found in southern Kuril Basin in Fig. 12 (a). This feature essentially agrees with the results of Runs 6 and 12 shown in Fig. 8 (a) and Fig. 9 (b), respectively, and it indicates that the circulation is considered as the western boundary circulation trapped in the offshore region by the effect of bottom slope. In Fig. 12 (b), a clear anti-cyclonic circulation is found in the northern Kuril Basin. This anti-cyclonic circulation is simulated in Runs 17 and 19 shown in Fig. 11 (b). It is suggested that the anti-cyclonic circulation is due to the retrogression of the inflow by the topograhic effect of the Kuril Basin. However, Fig. 12 (a) shows that prominent currents exist along the western coast of the Kamchatka Peninsula and eastern coast of Sakhalin. These currents have not simulated in the present models. There is a possibility that the these currents are formed by the baroclinic structure of the sea, which is not considered in the present model. It is suggested that inclusion of the density stratification is needed for the further step of modeling of the Okhotsk Sea.

Another shortcoming of the present study is the neglect of seasonal change in the in-and outflow corresponding to the Oyashio and the Soya Warm Current. As is shown in Figs. 8 and 9, the interaction between the wind-driven circulation and in- and outflow is one of essential process in the current system of the Okhotsk Sea. Therefore, the inclusion of the seasonal change in the in-and outflow in the model should be needed in the future study.

Acknowledgements

The authors would like to thank Drs. M. Aota, T. Takizawa and K. Ooshima of Hokkaido University and Mr. S. Mochizuti of Tokai University for their help and useful discussions on the present work.

References

1) KUTSUWADA, K. and K. SAKURAI. Climatological maps of wind stress field over the north Pacific. Oceanogr. Mag., 32: 25–46 (1982).
2) FAVORITE, F., A. J. DODIMEAD and K. NASU. Oceanography of the subarctic pacific Region, 1960–71. I. N. P. F. C., 33: 1–187 (1976).
3) AOTA, M. Studies on the Soya Warm Current (in Japanese). Low Temp. Sci. Ser. A, 33: 151–172 (1975).
4) AOTA, M. Oceanographic structure of the Soya Warm Current (in Japanese). Bull. Coast. Oceanogr., 22: 30–39 (1984).
5) TAKIZAWA, T. Characteristics of the Soya Warm Current in the Okhotsk Sea. J. Oceanogr. Soc. Japan, 38: 281–292 (1982).
6) KURASHINA, S. Water exhange in the Okhotsk Sea (in Japanese). Marine Sci., 18: 123–127 (1986).
7) KITANI, K. An oceanographic study of the Okhotsk Sea. Bull. Far Seas Res. Lab., 9: 45–77 (1973).
8) SUZUKI, K. and S. KANARI Tide in the Okhotsk Sea (in Japanese). Marine Sci., 18: 445–463 (1986).
9) PEDLOSKY, J. Geophysical Fluid Dynamics. Springer-Verlag, 624 pp. (1979).
10) MATSUNO, T. Numerical integration of the primitive equations by a simulated backward difference method. J. Meteor. Soc. Japan, 44: 76–84 (1966).
11) MUNK, W. On the wind-driven circulation. J. Meteorol., 7: 79–93 (1950).
12) SEKINE, Y. Wind-driven circulation in the Japan Sea and its influence on the branching of the Tsushima Current. Prog. Oceanogr., 17: 297-312 (1986).

13) MOCHIZUKI, S. and M. AOTA. Water mass transportation from the Okhotsk Sea to the Oyashio area. Proc. 3th Int. Sympo. Okhotsk Sea ice (in press).
14) MOROSHIKIN, K. B. A new surface current map in the Okhotsk Sea (in Russian). Okeanologia, 4: 614–643 (1964).

オホーツク海の風成海洋大循環に関する順圧数値モデル

関 根 義 彦

要旨：オホーツク海の風成海洋循環を順圧数値モデルを用いて調べた。風による海面応力は Kutsuwada and Sakurai[1] による1961年から1975年までの月別平均を用いた。数値モデルにより，オホーツク海の卓越した流れは比較的水深の大きい千島海盆周囲の陸棚斜面のみに制限されることが示された。さらに，夏はオホーツク海上での風の応力が小さいために風成循環は極めて弱く，主な流れは流入出によるのに対し，冬には風の応力が強く風成大循環が卓越することが示された。冬季の結氷の影響を調べるため，結氷しない領域にのみ風の応力を与えたモデルを試みた。その結果，北部の沿岸領域では流れが小さいものの，大半の領域ではロスビー波の伝播により流れが生じ非結氷域の風の影響を受けた循環ができることが示された。